Development 133, 631-640 doi:10.1242/dev.02225

XHas2 activity is required during somitogenesis and precursor cell migration in *Xenopus* development

Michela Ori[1], Martina Nardini[1], Paola Casini[1], Roberto Perris[2,3] and Irma Nardi[1,*]

In vertebrates, hyaluronan biosynthesis is regulated by three transmembrane catalytic enzymes denoted Has1, Has2 and Has3. We have previously cloned the *Xenopus* orthologues of the corresponding genes and defined their spatiotemporal distribution during development. During mammalian embryogenesis, Has2 activity is known to be crucial, as its abrogation in mice leads to early embryonic lethality. Here, we show that, in *Xenopus,* morpholino-mediated loss-of-function of *XHas2* alters somitogenesis by causing a disruption of the metameric somitic pattern and leads to a defective myogenesis. In the absence of *XHas2*, early myoblasts underwent apoptosis, failing to complete their muscle differentiation programme. XHas2 activity is also required for migration of hypaxial muscle cells and trunk neural crest cells (NCC). To approach the mechanism whereby loss of HA, following *XHas2* knockdown, could influence somitogenesis and precursor cell migration, we cloned the orthologue of the primary HA signalling receptor CD44 and addressed its function through an analogous knockdown approach. Loss of *XCD44* did not disturb somitogenesis, but strongly impaired hypaxial muscle precursor cell migration and the subsequent formation of the ventral body wall musculature. In contrast to *XHas2*, loss of function of *XCD44* did not seem to be essential for trunk NCC migration, suggesting that the HA dependence of NCC movement was rather associated with an altered macromolecular composition of the ECM structuring the cells' migratory pathways. The presented results, extend our knowledge on *Has2* function and, for the first time, demonstrate a developmental role for CD44 in vertebrates. On the whole, these data underlie and confirm the emerging importance of cell-ECM interactions and modulation during embryonic development.

KEY WORDS: Has2, CD44, Hyaluronan, Somitogenesis, Myogenesis, Cell migration, Neural crest, ECM, *Xenopus*

INTRODUCTION

Hyaluronan (HA) is a key glycosaminoglycan (GAG) of the embryonic ECM because of its recognized importance in the correct assembly of the interstitial matrices and its putative ability to influence cell behaviour through binding to signal transducing receptors, such as CD44 and RHAMM (Lesley et al., 2000; Turley et al., 2002; Toole, 2004). Additional cell regulatory functions of the GAG have been proposed to take place intracellularly (Lee and Spicer, 2000), but little is known about their significance. Early studies in the chick embryo strongly suggested that HA is central in creating migration-permissive microenvironments for the moving precursor cells, such as those of the peripheral nervous system, muscle and cartilage/bone (Perris et al., 1991; Perris and Perissinotto, 2000). Furthermore, the observed HA synthesis and secretion by the migrating precursor cells themselves suggest that pericellular accumulation of the GAG could favour the motile behaviour of the cells and potentially contribute to their correct homing by mediating important interactions with other ECM components (Perris, 1997; Perissinotto et al., 2000), or by triggering CD44-mediated signalling cascades (Ponta et al., 2003).

The vertebrate HA biosynthesis is governed by three catalytic enzymes that reside at the plasma membrane and are designated Has1, Has2 and Has3. The catalytic efficiency of these three enzymes seems to differ and the same applies to the composition of the HA product that they generate (Itano et al., 1999; Spicer and McDonald, 1998). In fact, HA polymers generated by *Has1* and *Has2* are of a similar size, reaching molecular weights of up to 2×10^6 Da, whereas *Has3* polymerizes shorter chains in the range of 2.5×10^5 Dalton. The precise biological significance of these diverse catalytic properties of the Has molecules is still not fully understood, nor it is known how the expression and activity of these enzymes may be regulated at the molecular and cellular level. Moreover, the three synthases are expressed in different temporal patterns during mouse development (Tien and Spicer, 2005) and in particular *Has2* has been identified as a major source of HA during initial organogenesis. Mice with a homozygous deletion of the *Has2* gene manifest severe cardiac and vascular abnormalities leading to death at midgestation (E9.5-10), underpinning a pivotal role of *Has2* during mammalian embryogenesis (Camenisch et al., 2000). The technical limitations in carrying out detailed analyses of the *Has2* gene function by transgenic approaches in rodents have incited analogous investigations in more accessible embryos, such as that of the fish and frog. Recently, downregulation of the *Has2* gene in zebrafish has been found to perturb the mesodermal cell movements responsible for the gastrulation process (Bakkers et al., 2004).

We and others have recently cloned the three known *Has* genes in *Xenopus laevis* and established their spatiotemporal distribution during early phases of development (Koprunner et al., 2000; Vigetti et al., 2003; Nardini et al., 2004). *XHas1*, *XHas2* and *XHas3* mRNAs are found to exhibit distinct and non-overlapping spatial expression patterns that differ significantly from those observed in zebrafish and which suggest an evolutionary divergence in the control of Has genes expression between tetrapods and teleosts. In particular, *XHas2* is mainly found in mesoderm-derived structures, such as developing myotomes and heart anlage, and it is expressed by premigratory trunk neural crest cells (NCC). Interestingly, expression of *XHas2* overlaps that of *MyoD* in cells committed to a muscle fate (Nardini et al.,

[1]Laboratori di Biologia Cellulare e dello Sviluppo, Dipartimento di Fisiologia e Biochimica, Università di Pisa, Via Carducci 13, Ghezzano, Pisa (PI) 56010, Italy. [2]Dipartimento di Biologia Evolutiva e Funzionale, Università di Parma, Viale delle Scienze 11/A Parma, (PR) 43100, Italy. [3]Divisione di Oncologia Sperimentale 2, Istituto Nazionale dei Tumori Aviano, CRO-IRCCS, Via Pedemontana Occidentale, 12, Aviano (PN) 33081, Italy.

*Author for correspondence (e-mail: inardi@dfb.unipi.it)

Accepted 28 November 2005

2004). These findings have prompted us to investigate the possible role of *XHas2* in somitogenesis, myogenic differentiation and trunk NCC migration, which, thus far, have not been possible to elucidate in *Has2*-null mice. To this end, we have also cloned the *Xenopus* orthologue of CD44, known to be the principal cell surface receptor of HA (Wheatley et al., 1993; Ponta et al., 2003) for which the precise role during vertebrate development still remains to be elucidated.

MATERIALS AND METHODS

Embryo manipulations and whole mount in situ hybridization

Xenopus laevis embryos obtained by hormone induced laying, were in vitro fertilized, dejelled, washed and incubated in 0.1×MMR. Embryos were staged according to Nieuwkoop and Faber (Nieuwkoop and Faber, 1967), fixed and stained for β-galactosidase (200-300 pg injected per embryo) as previously described (Sive et al., 2000) using alternatively a red or light-blue substrate for detection. Whole-mount in situ hybridization was performed on embryos fixed in MENFA according to standard procedures (Harland, 1991). Linearized plasmid from *MyoD* (HindIII/T7), *XCardiac Actin* (PvuII/Sp6), *Xp27* (BamHI/T7), *XPax3* (BglII/SP6), *XGremlin* (SalI/T3) were used to generate digoxigenin-11-UTP-labelled (Roche) antisense RNA probes from the polymerases indicated. BM purple (Roche) was used as substrate.

CD44 cloning and tissue distribution

The EST clone IMAGE:7008877 (NCBI GenBank Accession Number BC074228) was found to correspond to the *Xenopus* orthologue of *CD44* receptor. The EST clone was completely sequenced and the full cDNA sequence (NCBI GenBank Accession Number DQ143881) aligned with the vertebrate CD44 orthologues using the CLUSTALW (http://www.ebpac.uk./CLUSTALW) software. The *XCD44* cDNA sequence was found to correspond to the standard form of CD44. The coding region of *XCD44* was subcloned into the pGEM-T vector (Promega) and used for preparing RNA probe for in situ hybridization from the linearized plasmid (*Not*I/T7). RT-PCR analyses were performed on total RNA from *Xenopus* embryos isolated at different developmental stages, ranging from blastula to late tailbud. The corresponding cDNAs were prepared using ImProm-II Reverse Transcriptase (Promega). Amplification of the ornithine decarboxylase gene (ODC) has been used as internal control. The following primers were used: *XODC*, 5′-AATGGATTTCAGAGACCA-3′ (forward) and 5′-CCAAGGCTAAAGTTGCAG-3′ (reverse), 25 cycles; *XCD44*, 5′-CAAGCGCGTACAGTTATCAGC-3′ (forward) and 5′-TACAGAGTCTCCCTGGTATCC-3′ (reverse), 30 cycles.

Animal cap experiments

Embryos were injected in one blastomere at the two-cell stage with 100 pg of *activin* mRNA in vitro transcribed from an *activin* cDNA construct kindly provided by Jim Smith (University of Cambridge, UK), using the SP6 Cap Scribe kit (Roche). Activin-injected embryos were fixed at neurula stage and processed by whole-mount in situ hybridization to visualize *XHas2* expression. In a second set of experiments, animal caps were dissected out from stage 8-9 embryos in 1×MBS and, after healing, cultured in 0.5×MBS. Activin (Sigma) was directly added to the 0.5×MBS medium (100 μg/ml). Caps were incubated for 1-2 hours in presence of the morphogen, frozen in dry ice and subsequently processed for RNA extraction. Total RNA was isolated from animal caps of control and activin-treated embryos and the corresponding cDNAs were prepared using ImProm-II Reverse Transcriptase (Promega). For PCR amplification, the following primers were used: *XHas2*, 5′-ATGCACTGTGAACGGTTTATATGC-3′ (forward) and 5′-TCAAGCAAGCACCAAGTCATGTT-3′ (reverse), 31 cycles; *XBra*, 5′-TATATCCACCCAGACTCACCC-3′ (forward) and 5′-GATAGAGAGAGAGGTGCCCCG-3′ (reverse), 30 cycles; and ODC (ornithine decarboxylase), 5′-AATGGATTTCAGAGACCA-3′ (forward) and 5′-CCAAGGCTAA-AGTTGCAG-3′ (reverse), 26 cycles.

mRNA and morpholino injections

The complete coding sequence of *XHas2* was obtained by RT-PCR using the primers described above, on the basis of the sequence reported in NCBI GenBank (Accession Number AF168465). The PCR products were cloned into pGEM-T vector (Promega) and subsequently subcloned into the *Xho*I/*Stu*I sites of the CS2$^+$ vector. The full-length clone was completely sequenced and was found to be identical to the reported sequence for *XHas2* (Koprunner et al., 2000). Capped mRNAs were synthesized in vitro from nuc-β-gal (*Not*I/Sp6) (Chitnis et al., 1995) and from *XHas2*-CS2$^+$ (Asp718/Sp6), using the SP6 Cap Scribe kit (Roche). Sequences of the two non-overlapping *XHas2* antisense morpholino oligos were: *XHas2*-Mo1 (5′ non-translated region of the gene), 5′-GTTATTGCCTTGGTCCTGTGGTCAC-3′; *XHas2*-Mo2 (coding region from the start codon), 5′-TGCATATAAACCGTTCACAGTGCAT-3′. Sequences of the two non-overlapping *XCD44* antisense morpholino oligos were: *XCD44*-Mo1 (5′ non-translated region of the gene), 5′-TGTGCTCCGCAGACAAGAGGCTCCT-3′; *XCD44*-Mo2 (coding region from the start codon), 5′-TAACAATCCACAGCATTGAGGCCAT-3′. A control morpholino was synthesized as a random sequence of the same length (Gene Tools, Philomath, OR). Embryos were routinely co-injected with morpholino oligos and β-gal mRNA into one blastomere at the two-cell stage in 0.1×MMR supplemented with 4% Ficoll. Rescuing experiments were performed by injecting the optimal effective dose of *XHas2*-Mo1 (15 ng/embryo) in conjunction with *XHas2* mRNA (800-1000 pg/embryo) and β-gal mRNA.

Immunohistochemistry, BrdU incorporation and TUNEL staining

Whole-mount antibody staining was performed following standard procedures for indirect immunohistochemistry using an anti-muscle ATPase monoclonal antibody 12/101 (Developmental Studies Hybridoma Bank) at 1:10 dilution and HRP-conjugated secondary antibodies and DAB for detection. Immunostaining with the anti-phosphorylated H3 antibody was performed as described by Saka and Smith (Saka and Smith, 2001). BrdU incorporation and detection was performed essentially as previously described (Vernon and Philpott, 2003) and nuclei were counterstained with Hoechst. TUNEL staining for the identification of apoptotic cells was performed as described by Hensey and Gautier (Hensey and Gautier, 1998). After whole-mount TUNEL, *XHas2*-Mo injected neurula embryos were paraffin wax embedded and sectioned. The obtained slides were counterstained with Hoechst to allow the simultaneous visualization of normal and apoptotic nuclei.

Hyaluronan detection on tissue sections

Hyaluronan detection has been carried out using a Neurocan-GFP fusion protein kindly provided by Professor Uwe Rauch. Wild-type and *XHas2*-Mo injected embryos were fixed in 4% paraformaldehyde, paraffin wax embedded, processed for hyaluronan detection with the Neurocan-GFP probe essentially as described by Zhang et al. (Zhang et al., 2004), and counterstained with Hoechst.

RESULTS

XHas2 transcription is controlled by activin signalling during gastrulation

During *Xenopus* development, *XHas2* expression is first detected at gastrula stage in the involuting mesoderm and is subsequently seen in the paraxial mesoderm (Nardini et al., 2004). We find here that *XHas2* transcription is ectopically induced in *activin* mRNA-injected embryos in the ventrolateral region of the injected side demarcated by the co-injected β-gal (100%, *n*=50; Fig. 1A,A′). This finding indicates that *XHas2* is a downstream target of activin signalling and, hence, may be among the genes activated through mesoderm induction. In order to further investigate this, we compared the temporal expression profile of the *XBrachyury* gene, known to be a direct target of activin signalling, with that of *XHas2* in animal caps. The results reported in Fig. 1B show that *XHas2* transcription is activated within 1 hour of activin treatment presenting a time response behaviour similar to *XBrachyury*. This observation suggests that *XHas2* may be a direct target of activin signalling.

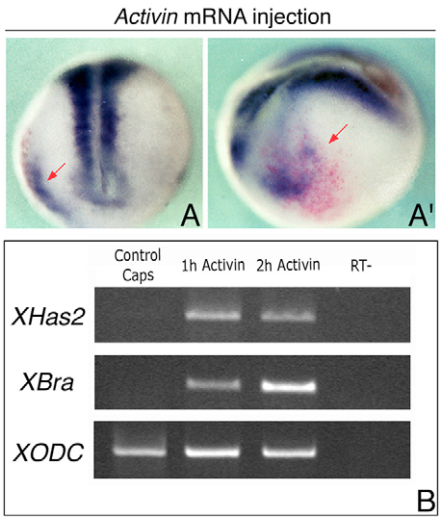

Fig. 1. *XHas2* is transcriptionally activated by activin. (**A,A'**) Ectopic *XHas2* mRNA expression in *activin*-injected embryos detected by whole-mount in situ hybridization. The site of injection is visualized by the Red-gal staining (red arrow). A, dorsal view; A′, lateral view. (**B**) Comparison of the expression profile of *XBrachyury* and *XHas2* in animal caps following activin treatment. *XODC* was used as positive control. RT- indicates representative samples of RNA from activin-treated animal caps, processed without reverse transcriptase and subsequently used as a negative control for *XHas2*, *XBrachyury* and *XODC* amplification.

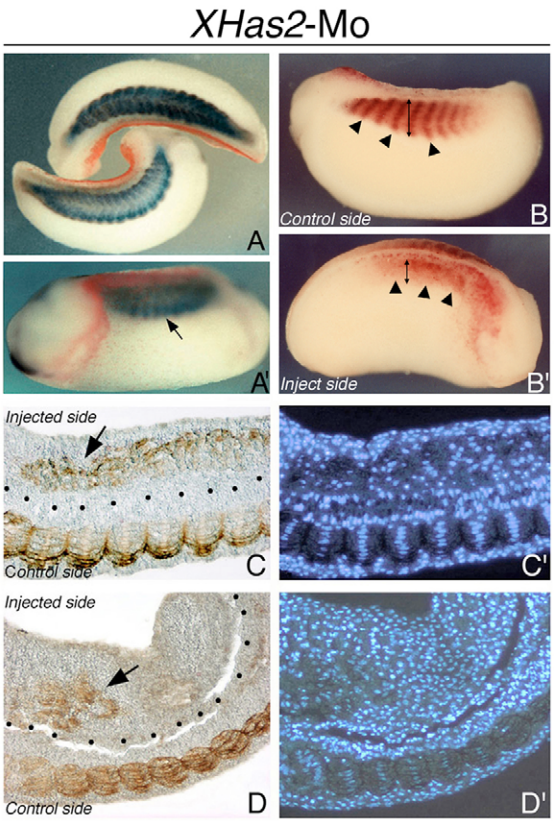

Fig. 2. Myotome alterations in *XHas2*-Mo injected embryos. All embryos are at stage 28-30 and are visualized by the expression of *CA* (A,A′) and by 12/101 immunoreactivity (B,B′,C,D). Red-gal staining identifies the injected side of the embryos. (**A**) Bending of the embryos was observed in the injected side. (**A'**) Example of a mild class phenotype embryo; the myotome arrangement is altered in the injected side of the embryo (arrow). (**B**) Lateral view of the control side of a representative case of a severe class phenotype at stage 26 (arrowheads indicate the somites). (**B'**) Injected side of the embryo in B showing a complete disruption of somites segmentation, as indicated by the arrowheads and a strong reduction in the 12/101-positive cells (compare double-headed arrows in B and B′). Red spots on the head and trunk region (Red-gal staining) identify the site of injection. (**C-D'**) Two representative cases of severe class phenotype embryos, longitudinally sectioned and stained with Hoechst to visualize the nuclei (C′,D′). (C,D) The pattern of the 12/101 positive myocytes is altered within the somites in the injected side (arrows).

XHas2 knockdown alters somitogenesis

In order to address the function of the *XHas2* during early phases of development, we used two different non-overlapping antisense morpholino oligos, *XHas2*-Mo1 and *XHas2*-Mo2. These were designed such as to be complementary to the *XHas2* mRNA sequence in a region surrounding the translational start codon. *XHas2* was targeted by injecting the morpholino oligos in one blastomere of *Xenopus* embryos at the two- or four-cell stages. The optimal morpholino concentration was established by independent pilot experiments and was determined to be in the range of 10-20 ng/embryo. At higher doses, the survival rate of the embryos decreased from 90-95% to 5-10% of the total number of injected embryos, whereas at lower doses we did not observe overt developmental defects. If not otherwise stated, all the experiments were performed by injecting both the morpholino oligonucleotides (indicated as *XHas2*-Mo) and β-gal mRNA in order to be able to select properly manipulated embryos on the basis of Salmon-gal or X-gal staining.

Knockdown of *XHas2* by injection of *XHas2*-Mo in one of the blastomeres of two-cell stage embryos did not affect gastrulation movements, but resulted in embryos bent towards the injected side by early tailbud stages (Fig. 2A-B′). Thus, we further investigated whether the manifested phenotype of *XHas2*-Mo-injected embryos could depend upon altered morphogenesis of the somites. *XHas2*-Mo-injected embryos were processed for in situ hybridization with a cardiac actin (*CA*) probe, or immunostained with the 12/101 antibody, a marker of terminal muscle differentiation. Myotome alterations were observed in 75% (n>100) of the embryos injected with 15-20 ng of *XHas2*-Mo (Fig. 2). The effect was reproducible, but relative penetrance of the phenotype differed between embryos that were therefore arbitrarily grouped into two main phenotype classes: those exhibiting mild and those exhibiting severe developmental abnormalities. In mild phenotypes, the somite tissue of the injected side was less abundant and had lost its canonical pattern, i.e. it did not have the chevron-like shape typical of somites at this developmental stage (tailbud stages). In these embryos, somite segmentation did not seem to be overtly affected (Fig. 2A′). By contrast, in severe class phenotypes, the segmental organization of the somites appeared disrupted in the injected side: individual somites had failed to segregate and no intersomitic boundaries were discernible (Fig. 2B-D′). During *Xenopus* somitogenesis, segmentation is accomplished by rotation of a block of cells by 90° and myotomal cells become dorsoventrally aligned. Tissue sections from injected embryos that were double stained with the 12/101 antibody and the nuclear dye Hoechst showed a failure of the somitic cells to rotate and align, causing most cells to remain in a disorganized mass (Fig. 2C′,D′). Moreover, the extension and

intensity of staining for the muscle-specific marker 12/101 was decreased in the injected side, suggesting that terminal muscle differentiation was inhibited (Fig. 2B′,C,D).

Specificity of the observed *XHas2*-Mo phenotypes was asserted by the following experiments. First, the two non-overlapping morpholino oligos were found to yield analogous developmental abnormalities when injected separately (not shown). Second, a morpholino oligonucleotide of the same length as the above ones, but with a random sequence, did not have any effect. This was ascertained by the normal expression pattern of *CA* in embryos selected for the presence of Red-gal staining in the somites (*n*=150; Fig. 3A). Third, the observed phenotypic abnormalities could effectively be rescued by co-injection of *XHas2*-Mo1 (complementary to the non-translated 5′-UTR region) and 800/1000 pg of *XHas2* mRNA. In fact, at tailbud stage, 76% of these embryos (*n*=80) developed normally (Fig. 3B-D). As seen in the *Has2* knockout mice (Camenisch et al., 2000), impaired heart formation was observed in *Xenopus* embryos that were injected with *XHas2*-Mo in the marginal zone of a dorsal blastomere at the four-cell stage and processed for *CA* in situ hybridization by stage 32. In 79% of these embryos (*n*=58), the heart anlage appeared highly abnormal (Fig. 3E,F). Abrogation of *XHas2* did not seem to cause overt compensatory (or collateral) effects on the expression pattern of *XHas1* and *XHas3* (not shown). The effective abrogation of XHas2 activity in the *XHas2*-Mo injected embryos has been verified visualizing the presence of HA on tissue sections. Recently, a new method has been proposed to detect HA on mice eye sections by means of a Neurocan-GFP fusion protein that specifically binds HA and directly visualizes it (Zhang et al., 2004). We first tested the Neurocan-GFP fusion protein on *Xenopus* embryos and then we visualized the presence of HA in *XHas2*-Mo-injected embryos at tailbud stage. As shown in Fig. 3, HA was abundant within the somitic ECM surrounding the myocytes. By comparing the control and injected side of the embryo, it was evident that the knockdown of *XHas2* caused a loss of HA in the myocyte pericellular matrix.

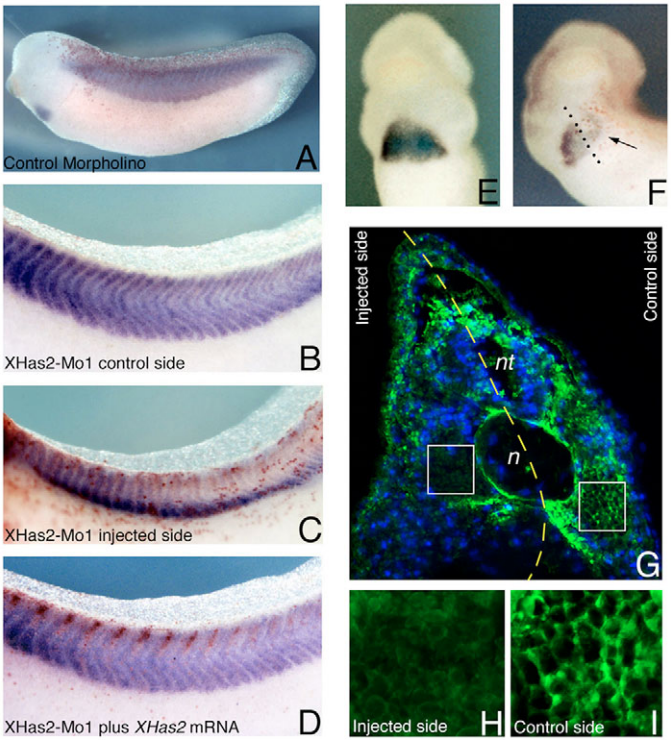

Fig. 3. Control experiments: stage 30 embryos were analyzed for *CA* expression and HA distribution. (**A**) A representative embryo injected with a control morpholino. (B-D) Embryos injected with 15 ng of *XHas2*-Mo1 or with 15 ng of *XHas2*-Mo1 plus 800 pg *XHas2* mRNA (rescue experiment). The injected side of the embryo is visualized by Red-gal staining. (**B**) Uninjected side of a *XHas2*-Mo1-injected embryo and (**C**) injected side of the same embryo showing the altered somites structure. (**D**) A representative case of a rescue experiment in which the canonical somites structure is completely recovered. (**E**) Ventral view of a wild-type embryo showing normal medial fusion of the two halves of the heart anlage. (**F**) In *XHas2*-Mo-injected embryos, heart formation is clearly impaired at the level of the injected side (arrow). (**G**) Coronal section of stage 26 *XHas2*-Mo-injected embryos at the trunk level and double stained with neurocan-GFP fusion protein (green) and Hoechst (blue). (**H**) High magnification of the *XHas2*-Mo-injected side region indicated by the white square in G; no HA detection is visible in the ECM surrounding the myocytes. (**I**) High magnification of the control side region indicated by the white square in G showing abundant HA in the ECM filling the myocytes extracellular spaces. n, notochord; nt, neural tube.

In order to identify the developmental time-window within which *XHas2*-generated HA was essential for somitogenesis, we analyzed the expression of early muscle-specific markers, such as *XMyoD* and *CA* at mid-neural plate stage, corresponding to the stage at which characteristic muscle-specific genes are first detected. In situ hybridization for *XMyoD* and *CA* in *XHas2*-Mo-injected embryos demonstrated that loss of *XHas2* function had no effect on *XMyoD* expression (*n*=175; Fig. 4A), whereas it severely affected the expression of *CA* in 70% of the embryos (*n*=111; Fig. 4B,B′). These findings suggest that HA synthesized through *XHas2* may not be required for myogenic specification, but is of relevance for the differentiation of presomitic mesodermal cells into muscle cells, probably by acting as a vital constituent of their surrounding ECM. To further explore this possibility, we examined neurula stage *XHas2*-Mo-injected embryos for the expression of *p27*, previously shown to be required for the cell-cycle exit of myoblasts and their completion of the muscle differentiation programme (Vernon and Philpott, 2003). In *XHas2*-Mo-injected embryos, expression of *p27* was indeed greatly reduced (65%, *n*=174), in a clear presomitic mesoderm-restricted manner, whereas it remained unaltered in primary neurons (Fig. 4C).

We next asked whether the downregulation of *p27* could be related to an altered proliferation, or to augmented apoptosis rate, in the presomitic mesoderm depleted of HA. To this end, we performed BrdU incorporation assays, immunohistochemistry with an anti-PH3 antibody and TUNEL assays to determine the relative levels of proliferating and apoptotic cells. We found that the amount of proliferating cells in the injected side of the neurula stage embryos was not significantly altered (*n*=80, Fig. 4E,F), whereas at the same stage, programmed cell death was greatly increased (70%, *n*=84, Fig. 4G,G′). Assessment of the relative percentage of apoptotic cells in paraxial mesoderm sections at neurula stage revealed that 30-40% of the presomitic cells were apoptotic in the injected side of the *XHas2*-Mo embryos (data not shown). In accordance, at early tailbud (stage 22), a clear reduction in the size of the forming somites was evident (Fig. 4D). When we carefully examined *XHas2*-Mo injected embryos at tailbud stages by TUNEL assay, we did not find any significant increase in the apoptotic rate in muscle cells, neither at stage 24 (*n*=52, Fig. 4H,H′) nor at stage 30 embryos (*n*=45; Fig. 4I,I′). In these embryos, a high level of apoptosis was normally found in the telencephalon with no differences between the injected

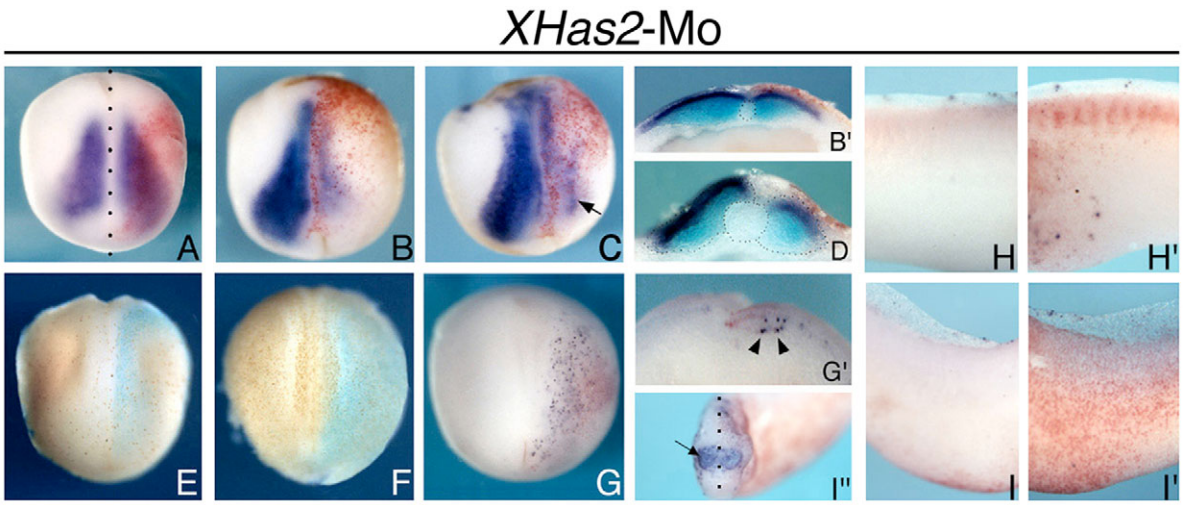

Fig. 4. *XHas2* loss-of-function phenotype during early myogenesis. Dorsal view of *XHas2*-Mo injected embryos at neurula stage analyzed for *XmyoD* (**A**), *CA* (**B,B′,D**) and *p27* (**C**) expression by whole-mount in situ hybridization. Notably, *p27* expression appeared unaltered in primary neurons (arrow). (B′) Bisection of embryo shown in B. (D) Bisected *XHas2*-Mo injected embryo at stage 22 showing a reduced somite mass in the injected side. (**E**) Injected neurula stage embryo stained with PH3 antibody. (**F**) Injected embryo analyzed by a BrdU incorporation assay (light blue, X-gal staining). (**G**) Whole mount TUNEL staining in *XHas2*-Mo injected neurula stage embryo. (**G′**) Bisected neurula embryo showing the increased number of apoptotic cells in the presomitic mesoderm of the injected side (*arrowheads*). (**H-I′**) Lateral view at the level of trunk somitic region of *XHas2*-Mo injected embryos processed by TUNEL assay. (H,I) Control side of stage 24 (H) and stage 30 (I) embryos. (H′,I′) Injected side of the embryos shown in H and I. No apoptotic cells were found at these stages in both control and injected side of the embryos. (**I′′**) In stage 30 embryos, physiological level of apoptosis was found in the telencephalon (arrow).

and the uninjected side of the embryo (Fig. 4I′′). It may therefore be concluded that *XHas2* activity plays a crucial role in preventing cells from apoptosis during a limited developmental time window that seems to concur with the early steps of myogenic differentiation.

Characterization and mRNA expression profile of XCD44

In order to shed light on the molecular mechanisms underling the HA/*XHas2* function during early embryogenesis, we cloned the *Xenopus* orthologue of the main hyaluronan receptor, CD44, and determined its expression pattern during development. Starting from an in silico screening using the human cDNA sequence of *CD44* we identified an EST clone (IMAGE ID: 4175501, partial sequence reported in GenBank: Accession Number BG657011) containing the putative *Xenopus CD44* orthologue. From the complete sequencing of this clone and a comparative analysis of the sequence with that of the known vertebrate *CD44* cDNAs, we were able to confirm that the identified clone corresponded to the standard form of the *Xenopus* hyaluronan receptor CD44 (XCD44). The deduced amino acid sequence of *XCD44* encompasses a characteristic link protein domain (residues 30-119), known to be responsible for hyaluronan binding, a consensus ERM (ezrin/radixin/moesin) protein-binding motif (residues 365-374) and a C-terminal putative binding site (KIVV) for class II PDZ proteins, similar to that found in the mammalian CD44 orthologues (Thorne et al., 2004).

The transcriptional profile of *XCD44* determined by RT-PCR analysis and whole-mount in situ hybridization showed that *XCD44* was first transcribed at early neurula stage (stage 13) and persisted until tadpole stage 45 (Fig. 5A). At late neurula stage, the *XCD44* transcript was detected in the presomitic mesoderm where it showed a segmental pattern that preceded the subsequent mesoderm segmentation and somite formation (Fig. 5B). By stage 24, *XCD44* was strongly expressed in the somites (Fig. 5C,C′) and in the cement gland, and at lower levels in the migrating cranial NCC (Fig. 5C). In tailbud embryos (stage 32), *XCD44* was transcribed in the somites, in the otic vesicle and in the branchial arches (Fig. 5D), whereas later on, it was found to be downregulated in the somitic tissue, except for the dorsal somite tips, and de novo expressed in the central nervous system, notochord and migrating hypaxial muscle cell precursors (Fig. 5E). Overall, the spatiotemporal gene expression pattern of *XCD44* largely overlapped that of *XHas2*, suggesting that the receptor could, at least in part, mediate the hyaluronan function during these stages of development.

XCD44 activity is not necessary for the early muscle differentiation and somitogenesis

Two non-overlapping morpholino oligos, *XCD44*-Mo1 and *XCD44*-Mo2, complementary to the 5′-end region of *XCD44*, were injected into one blastomere of *Xenopus* embryos at the two- or four-cell stages (15-20 ng/embryo). The downregulation experiments were performed by co-injecting a mixture of the two morpholino oligos (*XCD44*-Mo) that was found to yield a stronger effect and was consistently used throughout the study. β-Gal mRNA was injected with the *XCD44*-Mo in order to select properly manipulated embryos on the basis of the Salmon-gal or the X-gal staining. Morphological analysis of the injected embryos at tailbud stage did not reveal evident developmental abnormalities and in particular somite formation and segmentation seemed to be unaffected (Fig. 6D,D′). To detect possible alterations at cellular and molecular level in the injected side of the embryos, we further analyzed the expression of the genes involved in the early phases of myogenic commitment *MyoD* (n=56, Fig. 5F) and *p27* (n=53; Fig. 5G), and the specific differentiation marker *CA* (n=60; Fig. 5H). The expression pattern of these genes at neurula stage appeared unaffected. The TUNEL assay, performed at the same stage, did not reveal any increase in

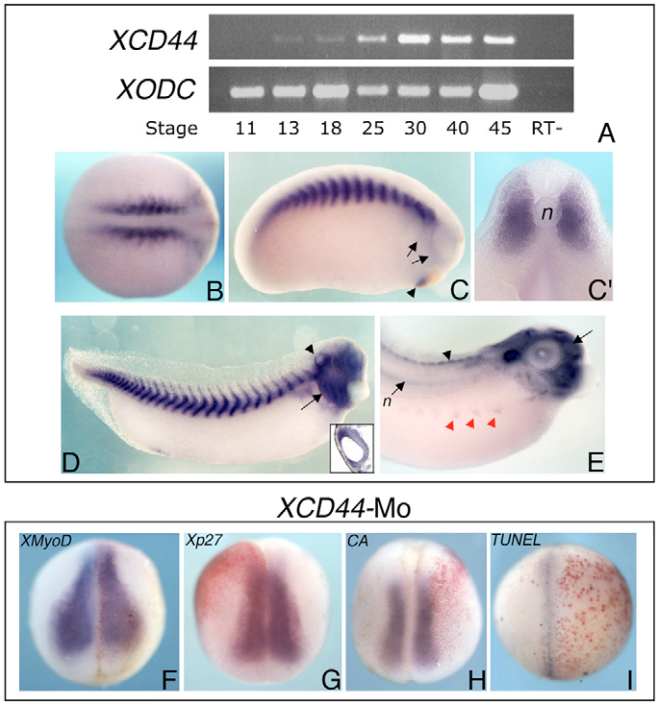

Fig. 5. *XCD44* gene expression pattern. (**A**) *XCD44* expression during *Xenopus* development analyzed by RT-PCR. (**B**) Dorsal view of a stage 20 embryo showing *XCD44* mRNA localization in the presomitic mesoderm. (**C**) Lateral view of a stage 24 embryo: *XCD44* gene expression is detected in somites, cement gland (arrowhead) and, at lower level, in the cranial NCC (arrows). (**C′**) Bisected embryo at stage 24 showing that in the trunk region *XCD44* is localized exclusively in the somites. The notochord (n) at this stage does not express *XCD44* mRNA. (**D**) Lateral view of stage 32 embryo: *XCD44* mRNA is present in somites, branchial arches (arrow) and in the otic vesicle (arrowhead). A horizontal section at the level of the otic region is shown in the inset. (**E**) Lateral view of a stage 37 embryo showing the localization of *XCD44* transcripts in the CNS (arrow), the dorsal somite tips (black arrowhead), the notochord and migrating hypaxial muscle cells (red arrowheads). (**F-H**) Dorsal view of *XCD44*-Mo injected embryos at neurula stage, the injected side of the embryos is visualized by the Red-gal staining. The expression of the following markers was detected by whole mount in situ hybridization: (F) *MyoD*, (G) *p27* and (H) *CA*. (**I**) An example of a *XCD44*-Mo injected embryo processed by TUNEL assay. The apoptotic cells are in blue; red spots indicate the site of injection.

the rate of apoptotic cells in the presomitic region of the injected side (n=68; Fig. 5I). These observations suggested that *XCD44* was not required for either early myogenesis or somite formation.

XHas2 and XCD44 are required for hypaxial muscle cell migration

During muscle formation, a specific cell population that originates from the ventral part of each somite migrates extensively to form the ventral body wall musculature. As HA has been suggested to be fundamental for embryonic cell movements, we asked whether loss of function of *XHas2* and/or *XCD44* could lead to an altered migration of these hypaxial muscle cells. In 66% of *XHas2*-Mo injected embryos (n=145), hypaxial muscle cell precursors appeared impaired in their ventral migration and remained confined to the ventral aspect of the somite (Fig. 6A-B′), or migrated less extensively, as determined by identification of the cells through *CA* hybridization and 12/101 antibody staining. Moreover, in *XHas2*-Mo injected embryos, we analyzed the expression of *XPax3*, known to be transiently upregulated in the ventral part of somites before hypaxial cells migration and then its expression is maintained in the migrating hypaxial muscle cells by stage 35-37 (Martin and Harland, 2001). In *XHas2*-Mo-injected embryos, *XPax3* expression persisted in the ventral part of somites and migrating hypaxial cells expressing *XPax3* were not detectable in the injected side of the embryo (68%, n=90; Fig. 6C,C′). These observations suggested that, when deprived of XHas2, hypaxial muscle cells were unable to commence their proper migration. A summary of the data obtained in *XHas2* and *XCD44* loss-of-function experiments during muscle development is reported in Table 1.

We next sought to define whether the HA/XHas2 role in muscle cells mobility was mediated by the XCD44-HA interaction. The 80% of the *XCD44*-Mo injected embryos analyzed at stage 37 by immunohistochemistry with the 12/101 antibody (n=95) showed an altered migratory pattern of hypaxial muscle cell precursors that was highly reminiscent of that observed in the *XHas2*-Mo injected embryos, while the trunk muscle mass seemed to develop normally (Fig. 6D,D′). To verify whether the hypaxial muscle cells were simply delayed in their migration or whether the ventral muscle formation was finally affected, we examined the ventral body wall muscles at stage 43 (Fig. 6E,E′) and found that 70% of the *XCD44*-Mo injected embryos indeed failed to develop a properly organized ventral musculature (n=64; Fig. 6F,F′). These embryos therefore recapitulated the *XHas2*-Mo phenotype observed at this stage of development (Fig. 6G,G′).

XHas2 knock down impairs trunk neural crest cell migration

As we have previously found that *XHas2* is expressed in premigratory trunk NCC (Nardini et al., 2004), we investigated here whether downregulation of the enzyme could also interfere with the migratory process of these precursor cells. *XHas2*-Mo-injected embryos were therefore hybridized with *XGremlin* to visualize migrating NCC (Hsu et al., 1998). In 70% (n=125) of these embryos, NCC failed to progress along their normal migratory pathways, resulting in randomly dispersed cells along the flank of the embryo, when compared with the control side (Fig. 7A-C). This observation did not allow us to discern if the detected phenotype was a direct consequence of the loss of *XHas2* activity in NCC, or a secondary alteration resulting from the abnormal development of somites in *XHas2*-Mo-injected embryos. In order to approach this aspect, we performed double in situ labelling of the somites, using the muscle-specific antibody 12/101 and the *XGremlin* probe to detect migrating NCC. Through this analysis, we could assert that the perturbation of NCC migration was consistently associated with the somitic mass reduction and segmentation abnormalities (n=120; Fig. 7D,D′). In accordance, *XHas2*-Mo-injected embryos exhibiting a mild muscle phenotype did not show an altered NCC migration. Although XCD44 is implicated in cell migration and mobility, *XCD44*-Mo-injected embryos did not show disturbed migration of trunk NCC (Fig. 7E,E′).

DISCUSSION

Deletion of the murine *Has2* gene causes early interruption of gestation due to severe cardiac defects (Camenisch et al., 2000). On one hand, this finding asserts the indispensable role of HA during embryonic development but, on the other hand, it leaves the precise role of the glycosaminoglycan during embryogenesis unresolved. To address this problem, we made use of a different vertebrate model in which functional abrogation of selected genes may be effectively performed in a more accessible embryo. Thus, after having

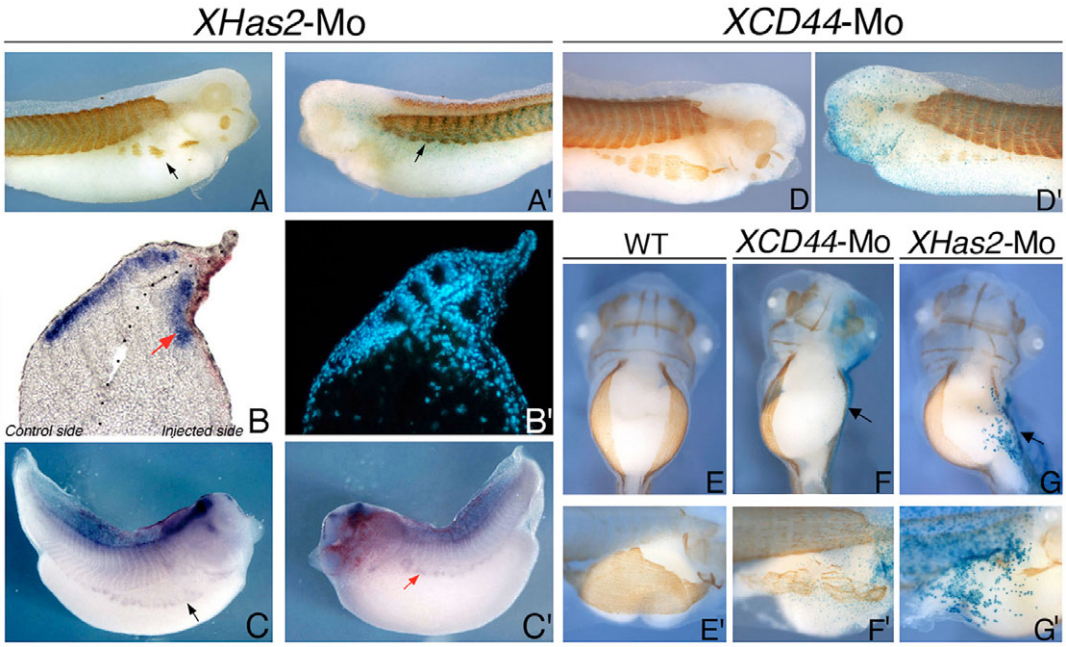

Fig. 6. Analysis of hypaxial cell migration in *XHas2*-Mo and *XCD44*-Mo injected embryos. (**A,A'**) Lateral view of control (A) and injected (A') side of an *XHas2*-Mo injected embryo (mild phenotype) at stage 37 showing the relative position of differentiating hypaxial muscle cells, as highlighted by 12/101 antibody staining (arrows). (**B,B'**) Transversally sectioned *XHas2*-Mo injected embryo hybridized with *CA* and coloured with Hoechst to visualize the nuclei, in which it is evident that the somite structure is altered and the ventrolateral migration of hypaxial muscle cells is impaired (red arrow). (**C**) Lateral view of the control side of a *XHas2*-Mo-injected embryo analyzed for *XPax3* expression by in situ hybridization at stage 37 highlighting hypaxial muscle cells migrating ventrally (arrow). (**C'**) Injected side of the embryo shown in C, in which hypaxial muscle cells are blocked at the ventral aspect of somites (red arrow). (**D,D'**) Stage 37 *XCD44*-Mo injected embryos immunostained with the 12/101 antibody. Although the trunk musculature appears unaffected by *XCD44* loss, migration of hypaxial cells is greatly reduced. (D) Control side of the embryo; (D') injected side. (**E-G**) Ventral views of stage 43 embryos immunostained with the 12/101 antibody that show the final position of the ventral body wall musculature in uninjected (E), *XCD44*-Mo injected embryo (F) and *XHas2*-Mo injected embryo (G). The side of injection is visualized by X-gal staining in blue and indicated by the arrow. (**E'-G'**) Lateral views of the same embryos shown in E-G, respectively.

accomplished the cloning and characterization of the expression pattern of the three known Has genes during *Xenopus* development (Vigetti et al., 2003; Nardini et al., 2004), we have addressed here the function of *XHas2* in the early developmental processes by exploiting a targeted knockdown approach at the post-transcriptional level. Our data highlight a crucial role of HA/*XHas2* in promoting survival and differentiation of myoblast cells, as well as in the somite formation. Our findings also assert a previously proposed key role for HA in mediating precursor cell migration with particular reference to muscle cell precursors of the ventral body wall and trunk NCC. Recently, a similar loss-of-function study performed in zebrafish embryos showed that *Has2* knockdown affected gastrulation (Bakkers et al., 2004). However, no gastrulation defects have been detected following *XHas2* knockdown in *Xenopus*, or deletion of the murine gene. This could in part be due to a complementary activity of *Has1*, which is found to be an early transcribed HA synthase both in *Xenopus* and mammals, but absent in the early zebrafish embryo. It may also be further speculated that such a developmentally related discrepancy in Has gene expression between tetrapods and teleosts may underlie a possible evolutionary divergence in the specific requirement of HA in different tissues and in specific time-windows of development.

During embryogenesis, HA is thought to play multiple roles in the regulation of cell behaviour which are brought about by its interaction with diverse ECM molecules, or via the direct activation of intracellular signal transductions mediated by

Table 1. Summary of the muscle phenotypes observed at different developmental stages in *XHas2* and *XCD44* loss of function experiments

	Stages 17-18		Stages 22-24		Stages 30-37	
	XHas2-Mo	*XCD44-Mo*	*XHas2-Mo*	*XCD44-Mo*	*XHas2-Mo*	*XCD44-Mo*
MyoD	*	*				
p27	–	*				
CA	–	*	–	*	–	*
Apoptotic rate	+	*	*	*	*	*
Muscle mass			–	*	–	*
Hypaxial cell migration					–	–

*, normal; –, reduced; + increased.
The number of processed embryos is provided in the text.

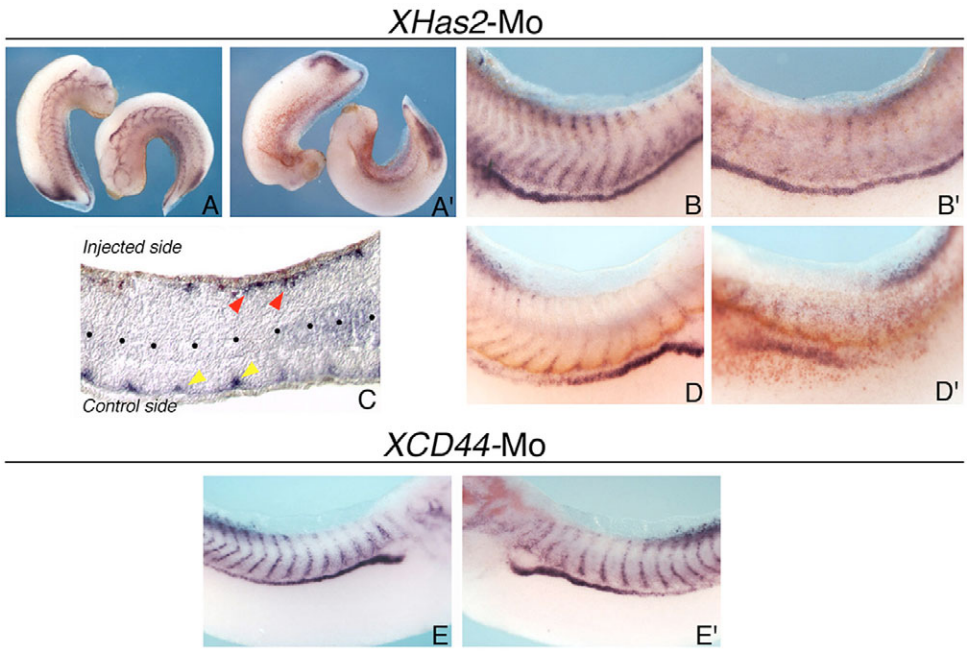

Fig. 7. Stage 32 *XHas2*-Mo and *XCD44*-Mo injected embryos analyzed for *XGremlin* expression by whole-mount in situ hybridization. (**A**) Lateral view of the control side of two embryos, showing NCC migration pathways. (**A′**) Lateral view of the injected side, revealed by Red-gal staining, of the embryos shown in A: no defined NCC migration pathways are recognizable. (**B**) Higher magnification of one of the embryo showed in A. (**B′**) Injected side of the embryo shown in B; NCCs are still present but they do not follow their normal migration routes. (**C**) Longitudinal section of an *XHas2*-Mo injected embryo: trunk NCCs appear dispersed along the somite external aspect (injected side, red arrowheads) instead of migrating along the intersomitic boundaries (control side, yellow arrowheads). (**D,D′**) Double-labelling of stage 32 embryo for *XGremlin* (blue) and 12/101 muscle-specific antigen (orange), whereas red staining reveals the injected side of the embryo. From the comparison of the control (D) and the injected sides (D′), it seems that the impairment of trunk NCC migration parallels the reduction and developmental alterations of somites. (**E,E′**) Stage 32 *XCD44*-Mo injected embryos analyzed for *XGremlin* expression. No differences in NCC migration are discernible between the control side (E) and the injected side (E′) of the embryo.

specific cell-surface receptors. Moreover, the analysis of the *Has2* role during mouse heart development has shown that HA is necessary for neuregulin binding and activation of Erb receptors (Camenisch et al., 2002). To better understand the possible mechanisms involved in the HA function during *Xenopus* somitogenesis and cell migration events, we cloned and analyzed the role of *CD44* during *Xenopus* development. So far, the localization of *CD44* transcripts during vertebrate development has not been reported and its role during embryogenesis is still unclear.

Activin is an upstream regulator of XHas2 transcriptional activation

The genetic cascade upstream of the transcriptional control of Has genes in vertebrates is completely unknown. We find that in accordance with its localization in the involuting mesoderm of the gastrula, *XHas2* expression is controlled by the activin signalling pathway, confirming that *XHas2* transcription is associated with mesoderm formation. Furthermore, as *XHas2* transcription is turned on within 1 hour of activin treatment of animal caps in vitro, it is tempting to suggest that *XHas2* may represent a novel direct target of activin signalling.

XHas2 but not XCD44 activity is required during early somitogenesis

Tailbud *Xenopus* embryos that received a unilateral injection of *XHas2* morpholino at the two-cell stage failed to correctly organize their flank musculature. In fact, in a mild version of the observed phenotype, embryos had smaller somites with a morphology deviating from the typical chevron-like arrangement observed in their normal counterparts. In severely affected phenotypes, the segmental organization of the myotomes appeared disrupted, with the individual somites remaining unsegregated and deprived of intersomitic boundaries. These observations raised the possibility that *XHas2* abrogation, could affect the structural integrity of the inter- and intra-somitic ECM, which in turn could have interfered with the establishment of correct cell-cell contacts between the forming myoblasts (Gurdon et al., 1993; Cossu et al., 1995). In situ analyses confirmed the decreased HA accumulation within the myocyte pericellular matrix as a consequence of the *XHas2* abrogation. It is also likely that this loss might has perturbed the intercellular connections that are thought to be crucial for proper formation of the somites, as cells normally undergo a coordinate 90° rotation and realign along the anteroposterior axis of the embryo (Keller, 2000).

As *XHas2* is expressed in the pre-somitic mesoderm, we asserted whether altered somitogenesis caused by loss of XHas2 activity was connected to an interference with the early phases of myogenic differentiation. When examined at neurula stage, *XHas2*-deprived embryos showed a significant loss of *CA* expression and a substantial increase in the apoptosis confined to the region where *XHas2* has been abrogated. Conversely, in the same area of the embryo, myoblast proliferation and the expression of the precocious muscle marker *MyoD* appeared unaffected. At the same developmental stage, we also detected a downregulation of *p27*, known to be a hallmark of the cell-cycle exit of myoblasts and their subsequent differentiation (Vernon and Philpott, 2003). These data strongly suggested that *XHas2* activity was not essential for the early myogenic commitment, or for myoblasts proliferation, but that it was required for the survival and differentiation of the early muscle precursors. Indeed, the role of *XHas2* in preventing these cells from undergoing apoptosis seems to be restricted to a specific developmental period, which coincides with the early steps of myogenic differentiation in the presomitic mesoderm. The effect of HA on survival and differentiation of presomitic mesodermal cells

could have been exerted through a structural supportive effect of the ECM, or alternatively HA produced by the myoblast cells could activate intracellular signals via binding to specific receptors such as CD44.

The pre-somitic expression of *XCD44* supported the above idea and was consistent with findings in other cellular systems showing that HA-mediated activation of CD44 exerts an anti-apoptotic effect through phosphorylation of FAK, activation of RhoB (Fujita et al., 2002) and upregulation of specific anti-apoptotic genes (Marhaba et al., 2003). However, abrogation of *XCD44* through morpholino injection revealed an unaffected early myogenesis and undisturbed formation of the trunk musculature at tailbud stages. Moreover, in *XCD44* morpholino-injected neurula embryos, there was no increase in apoptotic rate, suggesting that the *XHas2* generated HA prevented early myoblast death by a different mechanism than through CD44 signalling. However, proper assembly of the mesodermal ECM is likely to be required for bringing about community effects, for proper diffusion/gradient formation of morphogens, and/or for a normal action of other instructive signals responsible for the differentiation and survival of myogenic precursors. For example, it has been demonstrated that members of the TGFβ superfamily are more stable if complexed with HA, whereas they are rapidly degraded in matrices depleted of HA (Locci et al., 1995).

Comprehensively, our results suggest two possible scenarios for the HA/*XHas2* function during muscle development. First, HA/*XHas2* seem to have an early key role in the presomitic mesoderm where they support myoblast survival. *XHas2* depletion alters the muscle differentiation programme leading, in turn, to the development of embryos with strongly compromised somite arrangement. Second, the mild muscle phenotype observed in some of these embryos suggested an additional later role of *XHas2* in contributing to the formation of a hydrated ECM necessary for cell-cell contacts and morphogenetic movements. In this regard, it is interesting to note that the *XHas2* knockdown phenotype observed at tailbud stages was highly reminiscent of the one obtained by functional abrogation of type I cadherins (Giacomello et al., 2002), or paraxial proto-cadherins (Kim et al., 2000), which are cell adhesion molecules known to be essential for somitogenesis. The possibility to abrogate gene function in a time-regulated manner in *Xenopus*, or through conditional gene deletion in mice should allow the clarification of this aspect.

Hypaxial muscle cells migration is controlled by XHas2 and CD44 activity

In addition to its importance in trunk muscle cell development, *XHas2* appears to be involved in *Pax3*-positive hypaxial muscle cell migration which in *Xenopus* is crucial for the ventral body wall musculature formation (Martin and Harland, 2001). Pre-migratory expression of *XHas2* in these precursor cells suggests that the motility impairment, observed in the *XHas*-Mo-injected embryos, may, at least in part, be determined by the failure of these cells to produce HA during their locomotory process. This disturbed migratory pattern could be reconciled with a HA-mediated modulation of the cytoskeleton involved in cell motility and attributed to the engagement of CD44 linking to actin filaments through the ERM (ezrin, radixin and moesin) family proteins (Legg and Isacke, 1998). In breast cancer cell lines, HA has recently been shown to be capable of serving as a chemoattractant for directional migration in a CD44 activity-dependent manner probably via the intracellular association with ERM proteins (Tzircotis et al., 2005). As we find that the consensus binding motif for ERM proteins is conserved in the XCD44 orthologue and both this receptor and *XHas2* are co-expressed in hypaxial muscle precursor cells, it is likely that involvement of cytoskeletal components may be of relevance for the HA-XCD44 controlled migration of these precursor cells. The restricted alteration in cell motility in hypaxial muscle precursors following *XCD44* knockdown, raises an intriguing specific requirement of the receptor activity in a defined subpopulation of muscle cell precursors. In accordance, although the presence of CD44 has been detected in the mouse somites during development (Wheatley et al., 1993), neither the *CD44* gene deletion in mice (Protin et al., 1999) nor our post-transcriptional abrogation in *Xenopus* led to developmental abnormalities in the trunk musculature. The activity of alternative hyaluronan receptors during somites formation may be a possible explanation for this paradox.

Hyaluronan is crucial for proper trunk NCC migration

XHas2-deprived embryos showed altered trunk NCC migration, corroborating a proposed pivotal role of HA during NCC development (Perris et al., 1996; Perris, 1997; Perris and Perissinotto, 2000; Epperlein et al., 2000). In fact, previous experimental evidence from our group have indicated that different local accumulations of HA-versican complexes may define migration-permissive and non-permissive environments for NCC migrating in the trunk region of the embryo (Perris et al., 1991; Perissinotto et al., 2000). It is noteworthy that *Xenopus* migrating trunk NCC do not express *XCD44* and that depletion of the receptor in somitic cells does not influence the NCC movements. Although the presence of HA in the extracellular environment seems to be crucial for allowing proper NCC migration, it is not clear if the impaired movement of trunk NCC observed in *XHas2*-depleted embryos was due to a failure of these cells to synthesize and secrete HA, or to a structural deficit caused by its loss from the ECM of the NCC migratory pathways. An alternative possibility could be that the altered NCC migration could result from a morphogenetic loss of the structural integrity of the somites through which the cells migrate.

As a locally and temporally controlled tissue-specific knock-down of a gene is technically difficult to accomplish in *Xenopus*, we performed a double in situ labelling to simultaneously visualize muscle cell and migrating trunk NCC. Although further studies are needed to fully clarify this issue, the results suggest that defective NCC migration consistently coincides with areas of severe somitic malformation. This latter result may suggest that both a correct structure of somite and a HA enrichment of the ECM, contributed by NCC and myocytes, are necessary to create a specific environmental condition necessary to allow NCC migration. It is also plausible that there may be a different threshold requirement of *XHas2* activity in muscle cell precursors and NCC, whereby a partial loss of HA production may be sufficient to alter muscle formation (mild phenotype), but only a virtually complete depletion of matrix HA may interfere with both muscle development and NCC migration.

On the basis of our data, we suggest two different modes through which HA may govern cell migratory phenomena during embryogenesis: by directly influencing the migration process in cells expressing the HA receptor CD44, such as in the case of hypaxial cells; and by serving a structural function in the ECM through its linkage to different proteoglycans that may participate in the elaboration of permissive and non-permissive routes for NCC movement.

We thank Richard M. Harland, Jean-Paul Saint-Jeannet and William A. Harris for providing cDNA clones. We also thank Massimo Pasqualetti, Andrea Messina, Michelangelo Cordenonsi and Stefano Piccolo for their support in this project. We are particularly grateful to Uwe Rauch for the neurocan-GFP protein. Guglielma De Matienzo, Marzia Fabbri and Salvatore Di Maria are thanked for their technical assistance. The work was supported by grants from Agenzia Spaziale Italiana (ASI) and from the Ministero Italiano dell'Istruzione, dell'Università e della Ricerca (MIUR, Project: 'Functional analysis of the hyaluronan-hyaluronan receptor system during myogenesis and peripheral neurogenesis') and from Fondo Integrativo per la Ricerca di Base (FIRB, Project PRONEURO).

References

Bakkers, J., Kramer, C., Pothol, J., Quadvlieg, N. E. M., Spaink, H. P. and Hammerschmidt, M. (2004). Has2 is required upstream of Rac1 to govern dorsal migration of lateral cells during zebrafish gastrulation. *Development* **131**, 525-537.

Camenisch, T. D., Spider, A. P., Brehm-Gibson, T., Biesterfeldt, J., Augustine, M., Calabro, A., Kubalak, S., Klewer, S. and McDonald, J. A. (2000). Disruption of hyaluronan synthase-2 abrogates normal cardiac morphogenesis and hyaluronan-mediated transformation of epithelium to mesenchyme. *J. Clin. Invest.* **106**, 349-360.

Camenisch, T. D., Schroeder, J. A., Bradley, J. , Klewer, S. E. and McDonald, J. A. (2002). Heart-valve mesenchyme formation is dependent on hyaluronan-augmented activation of ErbB2-ErbB3 receptors. *Nat. Med.* **8**, 850-855.

Chitnis, A., Henrique, D., Lewis, J., Ish-Horowicz, D. and Kintner, C. (1995). Primary neurogenesis in *Xenopus* embryos regulated by a homologue of the Drosophila neurogenic gene Delta. *Nature* **375**, 761-766.

Cossu, G., Kelly, R., Di Donna, S., Vivarelli, E. and Buckingham, M. (1995). Myoblast differentiation during mammalian somitogenesis is dependent upon a community effect. *Proc. Natl. Acad. Sci. USA* **92**, 2254-2258.

Epperlein, H. H., Radomski, N., Wonka, F., Walther, P., Wilsch, M., Muller, M. and Schwarz, H. (2000). Immunohistochemical demonstration of hyaluronan and its possible involvement in axolotl neural crest cell migration. *J. Struct. Biol.* **132**, 19-32.

Fujita, Y., Kitagawa, M., Nakamura, S., Azuma, K., Ishii, G., Higashi, M., Kishi, H., Hiwasa, T., Koda, K., Nakajima, N. and Harigaya, K. (2002). CD44 signaling through focal adhesion kinase and its anti-apoptotic effect. *FEBS Lett.* **528**, 101-108.

Giacomello, E., Vallin, J., Morali, O., Coulter, I. S., Boulekbache, H., Thiery, J. P. and Broders, F. (2002). Type I cadherins are required for differentiation and coordinated rotation in Xenopus laevis somitogenesis. *Int. J. Dev. Biol.* **6**, 785-792.

Gurdon, J. B., Tiller, E., Roberts, J. and Kato, K. (1993). A community effect in muscle development. *Curr. Biol.* **3**, 1-11.

Harland, R. M. (1991). *In situ* hybridization, an improved whole mount method for *Xenopus* embryos. *Methods Cell Biol.* **36**, 685-695.

Hensey, C. and Gautier, J. (1998). Programmed cell death during *Xenopus* development, a spatio-temporal analysis. *Dev. Biol.* **203**, 36-48.

Hsu, D. R., Economides, A. N., Wang, X., Eimon, P. M. and Harland, R. M. (1998). The *Xenopus* dorsalizing Factor Gremlin identifies a novel family of secreted proteins that antagonize BMP activities. *Mol. Cell* **1**, 673-683.

Itano, N., Sawai, T., Yoshida, M., Lenas, P., Yamada, Y., Imagawa, M., Shinomura, T., Hamaguchi, M., Yoshida, Y., Ohnuki, Y. et al. (1999). Three isoforms of mammalian hyaluronan synthases have distinct enzymatic properties. *J. Biol. Chem.* **274**, 25085-25092.

Keller, R. (2000). The origin and morphogenesis of amphibian somites. *Curr. Top. Dev. Biol.* **47**, 183-246.

Kim, S. H., Jen, W. C., De Robertis, E. M. and Kintner, C. (2000). The protocadherin PAPC establishes segmental boundaries during somitogenesis in xenopus embryos. *Curr. Biol.* **10**, 821-830.

Koprunner, M., Mullegger, J. and Lepperdinger, G. (2000). Synthesis of hyaluronan of distinctly different chain length is regulated by differential expression of XHas1 and 2 during early development of *Xenopus laevis*. *Mech. Dev.* **90**, 275-278.

Lee, J. Y. and Spicer, A. P. (2000). Hyaluronan, a multifunctional, mega Dalton, stealth molecule. *Curr. Opin. Cell. Biol.* **12**, 581-586.

Legg, J. W. and Isacke, C. M. (1998). Identification and functional analysis of the ezrin-binding site in the hyaluronan receptor, CD44. *Curr. Biol.* **8**, 705-708.

Lesley, J., Hascall, V. C., Tammi, M. and Hyman, R. (2000). Hyaluronan binding by cell surface CD44. *J. Biol. Chem.* **275**, 26967-26975.

Locci, P., Marinucci, L., Lilli, C., Martinese, D. and Becchetti, E. (1995). Transforming growth factor beta 1-hyaluronic acid interaction. *Cell Tissue Res.* **1**, 317-324.

Marhaba, R., Bourouba, M. and Zoller, M. (2003). CD44v7 interferes with activation-induced cell death by up-regulation of anti-apoptotic gene expression. *J. Leukoc. Biol.* **74**, 135-148.

Martin, B. L. and Harland, R. M. (2001). Hypaxial muscle migration during primary myogenesis in *Xenopus laevis*. *Dev. Biol.* **239**, 270-280.

Nardini, M., Ori, M., Vigetti, D., Gornati, R., Nardi, I. and Perris, R. (2004). Regulated gene expression of hyaluronan synthases during *Xenopus laevis* development. *Gene Expr. Pattern.* **43**, 303-308.

Nieuwkoop, P. D. and Faber, J. (1967). *Normal Table of Development of Xenopus laevis (Daudin).* Amsterdam: North-Holland.

Perris, R. (1997). The extracellular matrix in neural crest cell migration. *TINS* **20**, 23-31.

Perris, R. and Perissinotto, D. (2000). Role of the extracellular matrix during neural crest cell migration. *Mech. Dev.* **95**, 3-21.

Perris, R., Krotoski, D., Lallier, T., Domingo, C., Sorrell, J. M. and Bronner-Fraser, M. (1991).Spatial and temporal distribution of proteoglycans during avian neural crest development. *Development* **111**, 583-599.

Perris, R., Perissinotto, D., Pettway, Z., Bronner-Fraser, M., Mörgelin, M. and Kimata, K. (1996). Inhibitory effect of the PG-H/aggrecan and PG-M/versican on avian neural crest cell migration. *FASEB J.* **10**, 293-301.

Perissinotto, D., Iacopetti, P., Bellina, I., Doliana, R., Colombatti, A., Pettway, Z., Bronner-Fraser, M., Shinomura, T., Kimata, K., Morgelin, M. et al. (2000). Avian neural crest cell migration is diversely regulated by the two major hyaluronan-binding proteoglycans PG-M/versican and aggrecan. *Development* **127**, 2823-2842.

Ponta, H., Sherman, L. and Herrlich, P. A. (2003). CD44: from adhesion molecules to signalling regulators. *Nat. Rev. Mol. Cell. Biol.* **4**, 33-45.

Protin, U., Schweighoffer, T., Jochum, W. and Hilberg, F. (1999). CD44-deficient mice develop normally with changes in subpopulations and recirculation of lymphocyte subsets. *J. Immunol.* **163**, 4917-4923.

Saka, Y. and Smith, J. C. (2001). Spatial and temporal patterns of cell division during early Xenopus embryogenesis. *Dev. Biol.* **229**, 307-318.

Sive, H., Grainger, R. and Harland, R. (2000). *Early Development of Xenopus laevis, A Laboratory Manual.* New York: Cold Spring Harbor Laboratory Press.

Spicer, A. P. and McDonald, J. A. (1998). Characterization and molecular evolution of a vertebrate hyaluronan synthase gene family. *J. Biol. Chem.* **273**, 1923-1932.

Thorne, R. F., Legg, J. W. and Isacke, C. M. (2004). The role of the CD44 transmembrane and cytoplasmic domains in co-ordinating adhesive and signalling events. *J. Cell Sci.* **117**, 373-380.

Tien, J. Y. and Spicer, A. P. (2005). Three vertebrate hyaluronan synthases are expressed during mouse development in distinct spatial and temporal patterns. *Dev. Dyn.* **233**, 130-141.

Toole, B. P. (2004). Hyaluronan: from extracellular glue to pericellular cue. *Nat. Rev. Cancer* **4**, 528-539.

Turley, E. A., Noble, P. W. and Bourguignon, L. Y. (2002). Signaling properties of hyaluronan receptors. *J. Biol. Chem.* **277**, 4589-4592.

Tzircotis, G., Thorne, R. F. and Isacke, C. M. (2005). Chemotaxis towards hyaluronan is dependent on CD44 expression and modulated by cell type variation in CD44-hyaluronan binding. *J. Cell Sci.* **118**, 5119-5128.

Vernon, A. and Philpott, A. (2003). A single cdk inhibitor, $p27^{xic1,}$ functions beyond cell cycle regulation to promote muscle differentiation in Xenopus. *Development* **130**, 71-83.

Vigetti, D., Viola, M., Gornati, R., Ori, M., Nardi, I., Passi, A., De Luca, G. and Bernardini, G. (2003). Molecular cloning, genomic organization and developmental expression of the *Xenopus laevis* hyaluronan synthase 3. *Matrix Biol.* **226**, 511-517.

Wheatley, S. C., Isacke, C. M. and Crossley, P. H. (1993). Restricted expression of the hyaluronan receptor, CD44, during postimplantation mouse embryogenesis suggests key roles in tissue formation and patterning. *Development* **119**, 295-306.

Zhang, H., Baader, S. L., Sixt, M., Kappler, J. and Rauch, U. (2004). Neurocan–GFP fusion protein: a new approach to detect hyaluronan on tissue sections and living cells. *J. Histochem. Cytochem.* **52**, 915-922.